arXiv:hep-ph/0303050v1 6 Mar 2003

An x-Space Analysis of Evolution Equations: Soffer's Inequality and the Non-forward Evolution

Alessandro Cafarella, Claudio Corianò and Marco Guzzi

Dipartimento di Fisica, Università di Lecce
and INFN Sezione di Lecce
Via Arnesano 73100 Lecce, Italy
and
alessandro.cafarella@le.infn.it, claudio.coriano@le.infn.it
marco.guzzi@le.infn.it

Abstract

We analize the use of algorithms based in x-space for the solution of renormalization group equations of DGLAP-type and test their consistency by studying bounds among partons distributions - in our specific case Soffer's inequality and the perturbative behaviour of the nucleon tensor charge - to next-to-leading order in QCD . A discussion of the perturbative resummation implicit in these expansions using Mellin moments is included. We also comment on the (kinetic) proof of positivity of the evolution of h_1, using a kinetic analogy and illustrate the extension of the algorithm to the evolution of generalized parton distributions. We prove positivity of the non-forward evolution in a special case and illustrate a Fokker-Planck approximation to it.

One of the most fascinating aspects of the structure of the nucleon is the study of the distribution of spin among its constituents, a topic of remarkable conceptual complexity which has gained a lot of attention in recent years. This study is entirely based on the classification and on the phenomenological modeling of all the leading-twist parton distributions, used as building blocks for further investigations in hadronic physics.

There are various theoretical ways to gather information on these non-local matrix elements. One among the various possibilities is to discover sum rules connecting moments of these distributions to other fundamental observables. Another possibility is to discover bounds - or inequalities - among them and use these results in the process of their modeling. There are various bounds that can be studied, particularly in the context of the new generalized parton dynamics typical of the skewed distributions [1, 2]. All these relations can be analized in perturbation theory and studied using the Renormalization Group (RG), although a complete description of their perturbative dynamics is still missing. This study, we believe, may require considerable theoretical effort since it involves a global understanding both of the (older) forward (DGLAP) dynamics and of the generalized new dynamics encoded in the skewed distributions.

In this context, a program aimed at the study of various bounds in perturbation theory using primarily a parton dynamics in x-space has been outlined [6]. This requires accurate algorithms to solve the equations up to next-to-leading order (NLO). Also, underlying this type of description is, in many cases, a probabilistic approach [3] which has some interesting consequences worth of a closer look . In fact, the DGLAP equation, viewed as a probabilistic process, can be rewritten in a *master form* which is at the root of some interesting formal developements. In particular, a wide set of results, available from the theory of stochastic processes, find their way in the study of the evolution. Two of us have elaborated on this issue in previous work [6] and proposed a Kramers-Moyal expansion of the DGLAP equation as an alternative way to describe its dynamics. Here, this analysis will be extended to the case of the non-forward evolution.

With these objectives in mind, in this study we test x-space algorithms up to NLO and verify their accuracy using a stringent test: Soffer's inequality. As usual, we are bound to work with specific models of initial conditions. The implementations on which our analysis are based are general, with a varying flavour number n_f at any threshold of intermediate quark mass in the evolution. Here, we address Soffer's inequality using an approach based on the notion of "superdistributions" [4], which are constructs designed to have a simple (positive) evolution thanks to the existence of an underlying master form [3, 6]. The original motivation for using such a master form (also termed *kinetic* or *probabilistic*) to prove positivity has been presented in [4], while further extensions of these arguments have been presented in [6]. In a final section we propose the extension of the evolution algorithm to the case of the skewed distributions, and illustrate its implementation in the non-singlet case. As for the forward case, numerical tests of the inequality are performed for two different models. We show that even starting from a saturated inequality at the lowest evolution scale, the various models differ significantly even for a moderate final factorization scale of $Q = 100$ GeV. Finally, we illustrate in another application the evolution of the tensor charge and show that, in the models considered, differences in the prediction of the tensor charge are large.

2 Prelude to x-space: A Simple Proof of Positivity of h_1 to NLO

There are some nice features of the parton dynamics, at least in the leading logarithmic approximation (LO), when viewed in x-space, once a suitable "master form" of the parton evolution equations is identified.

evolution equation itself. The topic has been addressed before in LO [4] and reanalized in more detail in [6] where, starting from a kinetic interpretation of the evolution, a differential equation obtained from the Kramers-Moyal expansion of the DGLAP equation has also been proposed.

The arguments of refs. [4, 6] are built around a form of the evolution equation which has a simple kinetic interpretation and is written in terms of transition probabilities constructed from the kernels.

The strategy used, at least in leading order, to demonstrate the positivity of the LO evolution for special combinations of parton distributions $\mathbf{Q}_\pm$ [4], to be defined below, or the NLO evolution for h_1, which we are going to address, is based on some results of ref.[4], briefly reviewed here, in order to be self-contained.

A master equation is typically given by

$$\frac{\partial}{\partial\tau}f(x,\tau) = \int dx' \left(w(x|x')f(x',\tau) - w(x'|x)f(x,\tau)\right) dx' \tag{1}$$

and if through some manipulations, a DGLAP equation

$$\frac{dq(x,Q^2)}{d\log(Q^2)} = \int_x^1 \frac{dy}{y} P(x/y)q(y,Q^2), \tag{2}$$

with kernels $P(x)$, is rewritten in such a way to resemble eq. (1)

$$\frac{d}{d\tau}q(x,\tau) = \int_x^1 dy\hat{P}\left(\frac{x}{y}\right)\frac{q(y,\tau)}{y} - \int_0^x \frac{dy}{y}\hat{P}\left(\frac{y}{x}\right)\frac{q(x,\tau)}{x}, \tag{3}$$

with a (positive) transition probability

$$w(x|y) = \frac{\alpha_s}{2\pi}\hat{P}(x/y)\frac{\theta(y>x)}{y} \tag{4}$$

then positivity of the evolution is established.

For equations of non-singlet type, such as those evolving $q^{(-)} = q - \bar{q}$, the valence quark distribution, or h_1, the transverse spin distribution, this rewriting of the equation is possible, at least in LO. NLO proofs are, in general, impossible to construct by this method, since the kernels turn out, in many cases, to be negative. The only possible proof, in these cases, is just a numerical one, for suitable (positive) boundary conditions observed by the initial form of the parton distributions. Positivity of the evolution is then a result of an unobvious interplay between the various contributions to the kernels in various regions in x-space.

In order to discuss the probabilistic version of the DGLAP equation it is convenient to separate the bulk contributions of the kernels ($x < 1$) from the edge point contributions at $x = 1$. For this purpose we recall that the structure of the kernels is, in general, given by

$$P(z) = \hat{P}(z) - \delta(1-z)\int_0^1 \hat{P}(z)\, dz, \tag{5}$$

where the bulk contributions ($z < 1$) and the edge point contributions ($\sim \delta(z-1)$) have been explicitely separated. We focus on the transverse spin distributions as an example. With these prerequisites, proving the LO and NLO positivity of the transverse spin distributions is quite straightforward, but requires a numerical inspection of the transverse kernels. Since the evolutions for $\Delta_T q^{(\pm)} \equiv h_1^q$ are purely non-singlet, diagonality in flavour of the subtraction terms ($\sim \int_0^x w(y|x)q(x,\tau)$) is satisfied, while the edge-point subtractions can be tested to be positive numerically. We illustrate the explicit construction of the master equation for h_1 in LO, since extensions to NLO of this construction are rather straighforward.

In this case the LO kernel is given by

$$\Delta_T P_{qq}^{(0)}(x) = C_F \left[\frac{2}{(1-x)_+} - 2 + \frac{3}{2}\delta(1-x) \right] \tag{6}$$

and by some simple manipulations we can rewrite the corresponding evolution equation in a suitable master form. That this is possible is an elementary fact since the subtraction terms can be written as integrals of a positive function. For instance, a possibility is to choose the transition probabilities

$$\begin{aligned} w_1[x|y] &= \frac{C_F}{y}\left(\frac{2}{1-x/y} - 2\right)\theta(y>x)\theta(y<1) \\ w_2[y|x] &= \frac{C_F}{x}\left(\frac{2}{1-y/x} - \frac{3}{2}\right)\theta(y>-x)\theta(y<0) \end{aligned} \tag{7}$$

which reproduce the evolution equation for h_1 in master form

$$\frac{dh_1}{d\tau} = \int_0^1 dy w_1(x|y)h_1(y,\tau) - \int_0^1 dy w_2(y|x)h_1(x,\tau). \tag{8}$$

The NLO proof of positivity is also rather straightforward. For this purpose we have analized numerically the behaviour of the NLO kernels both in their bulk region and at the edge-point. We show in Table 1 of Appendix B results for the edge point contributions to NLO for both of the $\Delta_T P_{\pm}^{(1)}$ components, which are numerically the same. There we have organized these terms in the form $\sim C\delta(1-x)$ with

$$C = -\log(1-\Lambda)A + B, \tag{9}$$

with A and B being numerical coefficients depending on the number of flavours included in the kernels. The (diverging) logarithmic contribution ($\sim \int_0^\Lambda dz/(1-z)$) have been regulated by a cutoff. This divergence in the convolution cancels when these terms are combined with the divergence at $x=1$ of the first term of the master equation (8) for all the relevant components containing "+" distributions. As for the bulk contributions ($x<1$), positivity up to NLO of the transverse kernels is shown numerically in Fig. (1). All the conditions of positivity are therefore satisfied and therefore the $\Delta_{T\pm}q$ distributions evolve positively up to NLO. The existence of a master form of the equation is then guaranteed.

Notice that the NLO positivity of $\Delta_{T\pm}q$ implies positivity of the nucleon tensor charge [5]

$$\delta q \equiv \int_0^1 dx \left(h_1^q(x) - h_1^{\bar{q}(x)} \right) \tag{10}$$

for each separate flavour for positive initial conditions. As we have just shown, this proof of positivity is very short, as far as one can check numerically that both components of eq.(8) are positive.

3 Soffer's inequality

Numerical tests of Soffer's inequality can be performed either in moment space or, as we are going to illustrate in the next section, directly in x-space, using suitable algorithms to capture the perturbative nature of the evolution. We recall that Soffer's inequality

$$|h_1(x)| < q^+(x) \tag{11}$$

sets a bound on the transverse spin distribution $h_1(x)$ in terms of the components of the positive helicity component of the quarks, for a given flavour. An original proof of Soffer's inequality in

interpretation of the evolution equations.

We recall that h_1, also denoted by the symbol

$$\Delta_T q(x,Q^2) \equiv q^{\uparrow}(x,Q^2) - q^{\downarrow}(x,Q^2), \tag{12}$$

has the property of being purely non-singlet and of appearing at leading twist. It is identifiable in transversely polarized hadron-hadron collisions and not in Deep Inelastic Scattering (from now on we will omit sometime the x-dependence in the kernels and in the distributions when obvious). In the following we will use interchangeably the notations $h_1 \equiv h_1^q$ and $\Delta_T q$ to denote the transverse asymmetries. We introduce also the combinations

$$\begin{aligned} \Delta_T(q+\bar{q}) &= h_1^q + h_1^{\bar{q}} \\ \Delta_T q^{(-)} = \Delta_T(q-\bar{q}) &= h_1^q - h_1^{\bar{q}} \\ \Delta_T q^{(+)} &= \sum_i \Delta_T(q_i + \bar{q}_i) \end{aligned} \tag{13}$$

where we sum over the flavor index (i), and we have introduced singlet and non-singlet contributions for distributions of fixed helicities

$$\begin{aligned} q_+^{(+)} &= \sum_i (q_{+i} + \bar{q}_{+i}) \\ q_+^{(-)} &= q_{+i} - \bar{q}_{+i} \equiv \Sigma. \end{aligned} \tag{14}$$

In our analysis we solve all the equations in the helicity basis and reconstruct the various helicities after separating singlet and non-singlet sectors. We mention that the non-singlet sector is now given by a set of 2 equations, each involving $\pm$ helicities and the singlet sector is given by a 4-by-4 matrix.

In the singlet sector we have

$$\begin{aligned} \frac{dq_+^{(+)}}{dt} &= \frac{\alpha_s}{2\pi}(P_{++}^{qq} \otimes q_+^{(+)} + P_{+-}^{qq} \otimes q_-^{(-)} \\ &\quad + P_{++}^{qG} \otimes G_+ + P_{+-}^{qG} \otimes G_-), \\ \frac{dq_-^{(+)}(x)}{dt} &= \frac{\alpha_s}{2\pi}(P_{+-} \otimes q_+^{(+)} + P_{++} \otimes q_-^{(+)} \\ &\quad + P_{+-}^{qG} \otimes G_+ + P_{++}^{qG} \otimes G_-), \\ \frac{dG_+(x)}{dt} &= \frac{\alpha_s}{2\pi}(P_{++}^{Gq} \otimes q_+^{(+)} + P_{+-}^{Gq} \otimes q_-^{(+)} \\ &\quad + P_{++}^{GG} \otimes G_+ + P_{+-}^{GG} \otimes G_-), \\ \frac{dG_-(x)}{dt} &= \frac{\alpha_s}{2\pi}(P_{+-}^{Gq} \otimes q_+^{(+)} + P_{++}^{Gq} \otimes q_-^{(+)} \\ &\quad + P_{+-}^{GG} \otimes G_+ + P_{++}^{GG} \otimes G_-). \end{aligned} \tag{15}$$

while the non-singlet (valence) analogue of this equation is also easy to write down

$$\begin{aligned} \frac{dq_{+i}^{(-)}(x)}{dt} &= \frac{\alpha_s}{2\pi}(P_{++}^{NS} \otimes q_{+i}^{(-)} + P_{+-}^{NS} \otimes q_-^{(-)}(y)), \\ \frac{dq_{-i}^{(-)}(x)}{dt} &= \frac{\alpha_s}{2\pi}(P_{+-}^{NS} \otimes q_+^{(-)} + P_{++}^{NS} \otimes q_{-i}^{(-)}). \end{aligned} \tag{16}$$

the helicity.

Similarly to the unpolarized case the flavour reconstruction is done by adding two additional equations for each flavour in the helicity $\pm$

$$\chi_{\pm,i} = q_{\pm i}^{(+)} - \frac{1}{n_f} q_{\pm}^{(+)} \tag{17}$$

whose evolution is given by

$$\begin{aligned} \frac{d\chi_{+i}^{(-)}(x)}{dt} &= \frac{\alpha_s}{2\pi}(P_{++}^{NS} \otimes \chi_{+i} + P_{+-}^{NS} \otimes \chi_{-i}), \\ \frac{d\chi_{-i}(x)}{dt} &= \frac{\alpha_s}{2\pi}(P_{+-}^{NS} \otimes \chi_{+i} + P_{++}^{NS} \otimes \chi_{-i}). \end{aligned} \tag{18}$$

The reconstruction of the various contributions in flavour space for the two helicities is finally done using the linear combinations

$$q_{\pm i} = \frac{1}{2}\left(q_{\pm i}^{(-)} + \chi_{\pm i} + \frac{1}{n_f} q_{\pm}^{(+)}\right). \tag{19}$$

We will be needing these equations below when we present a proof of positivity up to LO, and we will thereafter proceed with a NLO implementation of these and other evolution equations. For this we will be needing some more notations.

We recall that the following relations are also true to all orders

$$\begin{aligned} P(x) &= \frac{1}{2}\left(P_{++}(x) + P_{+-}(x)\right) \\ &= \frac{1}{2}\left(P_{--}(x) + P_{-+}(x)\right) \end{aligned}$$

between polarized and unpolarized (P) kernels and

$$P_{++}(x) = P_{--}(x), \;\; P_{-+}(x) = P_{+-}(x) \tag{20}$$

relating unpolarized kernels to longitudinally polarized ones. Generically, the kernels of various type are expanded up to NLO as

$$P(x) = \frac{\alpha_s}{2\pi} P^{(0)}(x) + \left(\frac{\alpha_s}{2\pi}\right)^2 P^{(1)}(x), \tag{21}$$

and specifically, in the transverse case we have

$$\Delta_T P_{qq,\pm}^{(1)} \equiv \Delta_T P_{qq}^{(1)} \pm \Delta_T P_{q\bar{q}}^{(1)} \,, \tag{22}$$

$$\tag{23}$$

with the corresponding evolution equations

$$\frac{d}{d\ln Q^2} \Delta_T q_{\pm}(Q^2) = \Delta_T P_{qq,\pm}(\alpha_s(Q^2)) \otimes \Delta_T q_{\pm}(Q^2) \,. \tag{24}$$

$$
\begin{aligned}
P^{(0)}_{NS\pm,++} &= P^{(0)}_{qq,++} = P^{(0)}_{qq} \\
P^{(0)}_{qq,+-} &= P^{(0)}_{qq,-+} = 0 \\
P^{(0)}_{qg,++} &= n_f x^2 \\
P_{qg,+-} &= P_{qg,-+} = n_f (x-1)^2 \\
P_{gq,++} &= P_{gq,--} = C_F \frac{1}{x} \\
P^{(0)}_{gg,++} &= P^{(0)}_{gg,++} = N_c \left(\frac{2}{(1-x)_+} + \frac{1}{x} - 1 - x - x^2 \right) + \beta_0 \delta(1-x) \\
P^{(0)}_{gg,+-} &= N_c \left(3x + \frac{1}{x} - 3 - x^2 \right).
\end{aligned} \tag{25}
$$

An inequality, such as Soffer's inequality, can be stated as positivity condition for suitable linear combinations of parton distributions [4] and this condition can be analized - as we have just shown for the h_1 case - in a most direct way using the master form.

For this purpose consider the linear valence combinations

$$
\begin{aligned}
\mathbf{Q}_+ &= q_+ + h_1 \\
\mathbf{Q}_- &= q_+ - h_1
\end{aligned} \tag{26}
$$

which are termed "superdistributions" in ref.[4]. Notice that a proof of positivity of the $\mathbf{Q}$ distributions is equivalent to verify Soffer's inequality. However, given the mixing of singlet and non-singlet sectors, the analysis of the master form is, in this case, more complex. As we have just mentioned, what can spoil the proof of positivity, in general, is the negativity of the kernels to higher order. We anticipate here the result that we will illustrate below where we show that a LO proof of the positivity of the evolution for $\mathbf{Q}$ can be established using kinetic arguments, being the kernels are positive at this order. However we find that the NLO kernels do not satisfy this condition. In any case, let's see how the identification of such master form proceeds in general. We find useful to illustrate the result using the separation between singlet and non-singlet sectors. In this case we introduce the combinations

$$
\begin{aligned}
\mathbf{Q}^{(-)}_\pm &= q^{(-)}_+ \pm h^{(-)}_1 \\
\mathbf{Q}^{(+)}_\pm &= q^{(+)}_+ \pm h^{(+)}_1
\end{aligned} \tag{27}
$$

with $h^{(\pm)}_1 \equiv \Delta_T q^{(\pm)}$.

Differentiating these two linear combinations (27) we get

$$
\frac{d\mathbf{Q}^{(-)}_\pm}{d\log(Q^2)} = P^{NS}_{++} q^{(-)}_+ + P^{NS}_{+-} q^{(-)}_- \pm P_T h^{(-)}_1 \tag{28}
$$

which can be rewritten as

$$
\begin{aligned}
\frac{d\mathbf{Q}^{(-)}_+}{d\log(Q^2)} &= \frac{1}{2}\left(P^{(-)}_{++} + P^{(-)}_T\right)\mathbf{Q}^{(-)}_+ + \frac{1}{2}\left(P^{(-)}_{++} - P^{(-)}_T\right)\mathbf{Q}^{(-)}_- + P^{(-)}_{+-} q^{(-)}_- \\
\frac{d\mathbf{Q}^{(-)}_+}{d\log(Q^2)} &= \frac{1}{2}\left(P^{(-)}_{++} - P^{(-)}_T\right)\mathbf{Q}^{(-)}_+ + \frac{1}{2}\left(P^{(-)}_{++} + P_T\right)^{(-)}\mathbf{Q}^{(-)}_- + P^{(-)}_{+-} q^{(-)}_-
\end{aligned} \tag{29}
$$

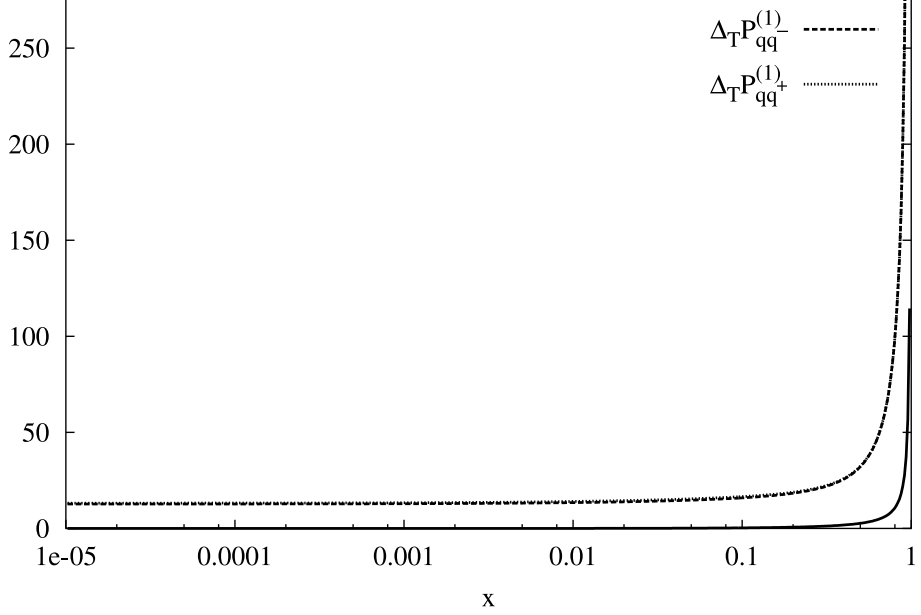

Figure 1: Plot of the transverse kernels.

with $P^{(-)} \equiv P^{NS}$ being the non-singlet (NS) kernel.

At this point we define the linear combinations

$$\bar{P}^Q_{+\pm} = \frac{1}{2}\left(P_{++} \pm P_T\right) \tag{30}$$

and rewrite the equations above as

$$\begin{aligned} \frac{d\mathbf{Q}_+ i}{d\log(Q^2)} &= \bar{P}^Q_{++}\mathbf{Q}_{i+} + \bar{P}^Q_{+-}\mathbf{Q}_{i-} + P^{qq}_{+-}q_{i-} \\ \frac{d\mathbf{Q}_{i+}}{d\log(Q^2)} &= \bar{P}^Q_{+-}\mathbf{Q}_{i+} + \bar{P}^Q_{++}\mathbf{Q}_{i-} + P^{qq}_{+-}q_{i-} \end{aligned} \tag{31}$$

where we have reintroduced i as a flavour index. From this form of the equations it is easy to establish the leading order positivity of the evolution, after checking the positivity of the kernel and the existence of a master form.

The second non-singlet sector is defined via the variables

$$\chi_{i\pm} = q^{(+)}_{i\pm} - \frac{1}{n_f} q^{(+)}_{i\pm} \tag{32}$$

which evolve as non-singlets and the two additional distributions

$$\mathbf{Q}_{\chi i,\pm} = \chi_{i+} \pm h^{i(+)}_1. \tag{33}$$

Also in this case we introduce the kernels

$$\bar{P}^{Q_\chi}_{+\pm} = \frac{1}{2}\left(P_{++} \pm \Delta_T P^{(+)}\right) \tag{34}$$

to obtain the evolutions

$$\begin{aligned} \frac{d\mathbf{Q}_{\chi i+}}{d\log(Q^2)} &= \bar{P}^{Q_\chi}_{++}\mathbf{Q}_{\chi i+} + \bar{P}^{Q_\chi}_{+-}\mathbf{Q}_{\chi i-} + P^{qq}_{+-}\chi_{i-} \\ \frac{d\mathbf{Q}_{i+}}{d\log(Q^2)} &= \bar{P}^{Q}_{\chi+-}\mathbf{Q}_{\chi i+} + \bar{P}^{Q_\chi}_{++}\mathbf{Q}_{\chi i-} + P^{qq}_{+-}\chi_{i-}. \end{aligned} \tag{35}$$

to the singlet equation of the helicity basis. Using the equations above, the distributions $\mathbf{Q}_{i\pm}$ are then reconstructed as

$$\mathbf{Q}_{i\pm} = \frac{1}{2}\left(\mathbf{Q}^{(-)}_{i\pm} + \mathbf{Q}^{(-)}_{\chi i\pm} + \frac{1}{n_f}Q^{(+)}_{+}\right) \tag{36}$$

and result positive for any flavour if the addends are positive as well. However, as we have just mentioned, positivity of all the kernels introduced above is easy to check numerically to LO, together with their diagonality in flavour which guarantees the existence of a master form.

As an example, consider the LO evolution of $\mathbf{Q}\pm$. The proof of positivity is a simple consequence of the structure of eq. (31). In fact the edge-point contributions appear only in P^{Q}_{++}, i.e. they are diagonal in the evolution of $\mathbf{Q}_{\pm}$. The inhomogenous terms on the right hand side of (31), proportional to q_- are are harmless, since the P_{+-} kernel has no edge-point contributions. Therefore under 1) diagonality in flavour of the subtraction terms and 2) positivity of first and second term (transition probabilities) we can have positivity of the evolution. A refined arguments to support this claim has been presented in [6].

This construction is not valid to NLO. In fact, while the features of flavour diagonality of the master equation are satisfied, the transition probabilities $w(x,y)$ are not positive in the whole x, y range. The existence of a crossing from positive to negative values in $P^{\mathbf{Q}}_{++}$ can, in fact, be established quite easily using a numerical analysis. We illustrate in Figs. (2) and (3) plots of the $\mathbf{Q}$ kernels at LO and NLO, showing that, at NLO, the requirement of positivity of some components is violated. The limitations of this sort of proofs -based on kinetic arguments- are strictly linked to the positivity of the transition probabilities once a master form of the equation is identified.

4 An x-space Expansion

We have seen that NLO proofs of positivity, can be -at least partially- obtained only for suitable sets of boundary conditions. To this purpose, we choose to investigate the numerical behaviour of the solution using x-space based algorithms which need to be tested up to NLO.

Our study validates a method which can be used to solve evolution equations with accuracy in leading and in next-to-leading order. The method is entirely based on an expansion [15] used in the context of spin physics [8] and in supersymmetry [9]. An interesting feature of the expansion, once combined with Soffer's inequality, is to generate an infinite set of relations among the scale invariant coefficients (A_n, B_n) which characterize it.

In this approach, the NLO expansion of the distributions in the DGLAP equation is generically given by

$$f(x,Q^2) = \sum_{n=0}^{\infty}\frac{A_n(x)}{n!}\log^n\left(\frac{\alpha(Q^2)}{\alpha(Q_0^2)}\right) + \alpha(Q^2)\sum_{n=0}^{\infty}\frac{B_n(x)}{n!}\log^n\left(\frac{\alpha(Q^2)}{\alpha(Q_0^2)}\right) \tag{37}$$

where, to simplify the notation, we assume a short-hand matrix notation for all the convolution products. Therefore $f(x,Q^2)$ stands for a vector having as components any of the helicities of the various flavours $(\mathbf{Q}_{\pm}, q_{\pm}, G_{\pm})$. The ansatz implies a tower of recursion relations once the running coupling is kept into account and implies that

$$A_{n+1}(x) = -\frac{2}{\beta_0}P^{(0)}\otimes A_n(x) \tag{38}$$

to leading order and

$$\begin{aligned} B_{n+1}(x) &= -B_n(x) - \left(\frac{\beta_1}{4\beta_0}A_{n+1}(x)\right) - \frac{1}{4\pi\beta_0}P^{(1)}\otimes A_n(x) - \frac{2}{\beta_0}P^{(0)}\otimes B_n(x) \\ &= -B_n(x) + \left(\frac{\beta_1}{2\beta_0^2}P^{(0)}\otimes A_n(x)\right) \end{aligned}$$

$$4\pi\beta_0 \qquad\qquad \beta_0 \tag{39}$$

to NLO, relations which are solved with the initial condition $B_0(x) = 0$. The initial conditions for the coefficients $A_0(x)$ and $B_0(x)$ are specified with $q(x, Q_0^2)$ as a leading order ansatz for the initial distribution

$$A_0(x) = \delta(1-x) \otimes q(x, Q_0^2) \equiv q_0(x) \tag{40}$$

which also requires $B_0(x) = 0$, since we have to satisfy the boundary condition

$$A_0(x) + \alpha_0 B_0(x) = q_0(x). \tag{41}$$

Again, other boundary choices are possible for $A_0(x)$ and $B_0(x)$ as far as (41) is fullfilled.

If we introduce Rossi's expansion for h_1, q_+, and the linear combinations $\mathbf{Q}_\pm$ (in short form)

$$\begin{aligned} h_1 &\sim \left(A_n^h, B_n^{h+}\right) \\ q_\pm &\sim (A_n^{q\pm}, B_n^{q\pm}) \\ \mathbf{Q}_\pm &\sim \left(A_n^{Q+}, B_n^{Q+}\right) \end{aligned} \tag{42}$$

we easily get the inequalities

$$(-1)^n \left(A_n^{q+} + A_n^h\right) > 0 \tag{43}$$

and

$$(-1)^n \left(A_n^{q+} - A_n^h\right) > 0 \tag{44}$$

valid to leading order,which we can check numerically. Notice that the signature factor has to be included due to the alternation in sign of the expansion. To next to leading order we obtain

$$(-1)^{n+1} \left(A_n^{q+}(x) + \alpha(Q^2) B_n^{q+}(x)\right) < (-1)^n \left(A_n^h(x) + \alpha(Q^2) B_n^h(x)\right) < (-1)^n \left(A_n^{q+}(x) + \alpha(Q^2) B_n^{q+}(x)\right), \tag{45}$$

valid for $n \geq 1$, obtained after identification of the corresponding logarithmic powers $\log(\alpha(Q^2))$ at any Q. In general, one can assume a saturation of the inequality at the initial evolution scale

$$\mathbf{Q}_-(x, Q_0^2) = h_1(x, Q_0^2) - \frac{1}{2} q_+(x, Q_0^2) = 0. \tag{46}$$

This initial condition has been evolved in Q solving the equations for the $\mathbf{Q}_\pm$ distributions to NLO.

5 Relations among moments

In this section we elaborate on the relation between the coefficients of the recursive expansion as defined above and the standard solution of the evolution equations in the space of Mellin moments. We will show that the two solutions can be related in an unobvious way.

Of our concern here is the relation between the Mellin moments of the coefficients appearing in the expansion

$$\begin{aligned} A(N) &= \int_0^1 dx\, x^{N-1} A(x) \\ B(N) &= \int_0^1 dx\, x^{N-1} B(x) \end{aligned} \tag{47}$$

$$\Delta_T q_\pm(N,Q^2) = \int_0^1 dx\, x^{N-1} \Delta_T(x,Q^2)). \tag{48}$$

For this purpose we recall that the general (non-singlet) solution to NLO for the latter moments is given by

$$\Delta_T q_\pm(N,Q^2) \;=\; K(Q_0^2,Q^2,N) \left(\frac{\alpha_s(Q^2)}{\alpha_s(Q_0^2)}\right)^{-2\Delta_T P_{qq}^{(0)}(N)/\beta_0} \Delta_T q_\pm(N,Q_0^2)$$

with the input distributions $\Delta_T q_\pm^n(Q_0^2)$ at the input scale Q_0 and where we have set

$$K(Q_0^2,Q^2,N) = 1 + \frac{\alpha_s(Q_0^2)-\alpha_s(Q^2)}{\pi\beta_0}\left[\Delta_T P_{qq,\pm}^{(1)}(N) - \frac{\beta_1}{2\beta_0}\Delta_T P_{qq\pm}^{(0)}(N)\right]. \tag{49}$$

In the expressions above we have introduced the corresponding moments for the LO and NLO kernels ($\Delta_T P_{qq}^{(0),N}$, $\Delta_T P_{qq,\pm}^{(1),N}$).

We can easily get the relation between the moments of the coefficients of the non-singlet x-space expansion and those of the parton distributions at any Q, as expressed by eq. (49)

$$A_n(N) + \alpha_s B_n(N) = \Delta_T q_\pm(N,Q_0^2) K(Q_0,Q,N) \left(\frac{-2\Delta_T P_{qq}(N)}{\beta_0}\right)^n. \tag{50}$$

As a check of this expression, notice that the initial condition is easily obtained from (50) setting $Q \to Q_0, n \to 0$, thereby obtaining

$$A_0^{NS}(N) + \alpha_s B_0^{NS}(N) = \Delta_T q_\pm(N,Q_0^2) \tag{51}$$

which can be solved with $A_0^{NS}(N) = \Delta_T q_\pm(N,Q_0^2)$ and $B_0^{NS}(N) = 0$.

It is then evident that the expansion (37) involves a resummation of the logarithmic contributions, as shown in eq. (50).

In the singlet sector we can work out a similar relation both to LO

$$A_n(N) = e_1 \left(\frac{-2\lambda_1}{\beta_0}\right)^n + e_2 \left(\frac{-2\lambda_2}{\beta_0}\right)^n \tag{52}$$

with

$$\begin{aligned}
e_1 &= \frac{1}{\lambda_1-\lambda_2}\left(P^{(0)}(N) - \lambda_2 \mathbf{1}\right) \\
e_2 &= \frac{1}{\lambda_2-\lambda_1}\left(-P^{(0)}(N) + \lambda_1 \mathbf{1}\right) \\
\lambda_{1,2} &= \frac{1}{2}\left(P_{qq}^{(0)}(N) + P_{gg}^{(0)}(N) \pm \sqrt{\left(P_{qq}^{(0)}(N) - P_{gg}^{(0)}(N)\right)^2 + 4P_{qg}^{(0)}(N)P_{gq}^{(0)}(N)}\right),
\end{aligned} \tag{53}$$

and to NLO

$$A_n(N) + \alpha_s B_n(N) = \chi_1 \left(\frac{-2\lambda_1}{\beta_0}\right)^n + \chi_2 \left(\frac{-2\lambda_2}{\beta_0}\right)^n \tag{54}$$

where

$$\begin{aligned}
\chi_1 &= e_1 + \frac{\alpha}{2\pi}\left(\frac{-2}{\beta_0} e_1 \mathbf{R} e_1 + \frac{e_2 \mathbf{R} e_1}{\lambda_1-\lambda_2-\beta_0/2}\right) \\
\chi_2 &= e_2 + \frac{\alpha}{2\pi}\left(\frac{-2}{\beta_0} e_2 \mathbf{R} e_2 + \frac{e_1 \mathbf{R} e_2}{\lambda_2-\lambda_1-\beta_0/2}\right)
\end{aligned} \tag{55}$$

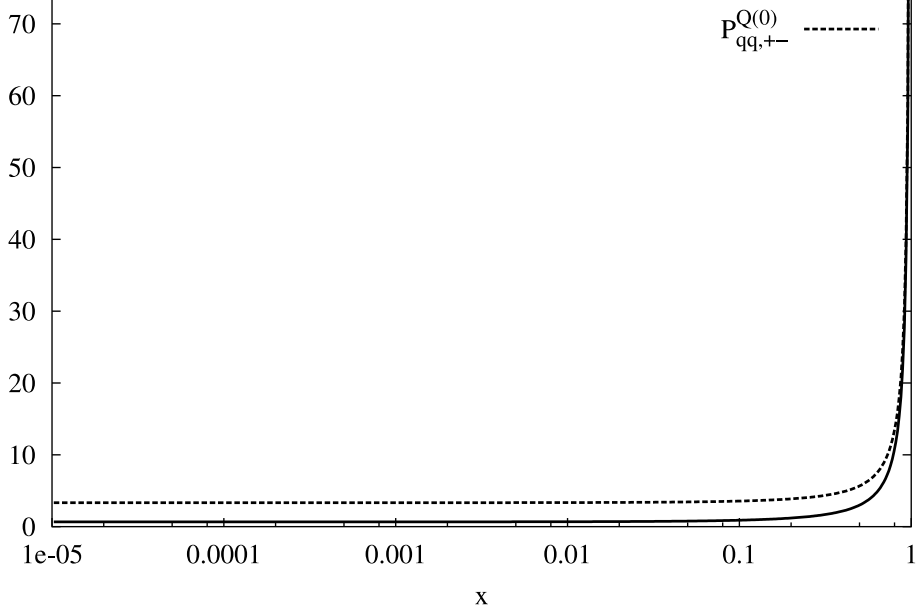

Figure 2: Plot of the LO kernels for the **Q** distributions

with

$$\mathbf{R} = P^{(1)}(N) - \frac{\beta_1}{2\beta_0} P^{(0)}(N). \tag{56}$$

Notice that $A_n(N)$ and $B_n(N)$, $P^{(0)}(N)$, $P^{(1)}(N)$, in this case, are all 2-by-2 singlet matrices. Prior to discuss some phenomenological application of this method, left to a final section, we will now illustrate its application to the case of the evolution of h_1 up to NLO. Its extension to the case of the generalized parton distributions will follow afterwards.

6 An Example: The Evolution of the Transverse Spin Distributions

LO and NLO recursion relations for the coefficients of the expansion can be worked out quite easily, although the numerical implementation of these equations is far from being obvious. Things are somehow simpler to illustrate in the case of simple non-singlet evolutions, such as those involving transverse spin distributions, as we are going to show below. Some details and definitions can be found in the appendix.

For the first recursion relation (eq. (38)) we have

$$\begin{aligned} &A_{n+1}^{\pm}(x) = -\frac{2}{\beta_0}\Delta_T P_{qq}^{(0)}(x) \otimes A_n^{\pm}(x) = \\ &C_F\left(-\frac{4}{\beta_0}\right)\left[\int_x^1 \frac{dy}{y}\frac{yA_n^{\pm}(y) - xA_n^{\pm}(x)}{y-x} + A_n^{\pm}(x)\log(1-x)\right] + \\ &C_F\left(\frac{4}{\beta_0}\right)\left(\int_x^1 \frac{dy}{y}A_n^{\pm}(y)\right) + C_F\left(-\frac{2}{\beta_0}\right)\frac{3}{2}A_n^{\pm}(x)\,. \end{aligned} \tag{57}$$

As we move to NLO, it is convenient to summarize the structure of the transverse kernel $\Delta_T P_{qq}^{\pm,(1)}(x)$ as

$$\Delta_T P_{qq}^{\pm,(1)}(x) = K_1^{\pm}(x)\delta(1-x) + K_2^{\pm}(x)S_2(x) + K_3^{\pm}(x)\log(x)$$

Hence, for the (+) case we have

$$\Delta_T P_{qq}^{+,(1)}(x) \otimes A_n^+(x) = K_1^+ A_n^+(x) + \int_x^1 \frac{dy}{y} \left[K_2^+(z) S_2(z) + K_3^+(z) \log(z) \right.$$
$$\left. + \log^2(z) K_4^+(z) + \log(z) \log(1-z) K_5^+(z) \right] A_n^+(y) +$$
$$K_6^+ \left\{ \int_x^1 \frac{dy}{y} \frac{y A_n^+(y) - x A_n^+(x)}{y-x} + A_n^+(x) \log(1-x) \right\} + K_7^+ \int_x^1 \frac{dy}{y} A_n^+(y) \,, \tag{59}$$

where $z = x/y$. For the $(-)$ case we get a similar expression.

Now we are ready to write down the expression for the $B_{n+1}^{\pm}(x)$ coefficient to NLO, similarly to eq. (39). So we get (for the (+) case)

$$B_{n+1}^+(x) = -B_n^+(x) + \frac{\beta_1}{2\beta_0^2} \left\{ 2C_F \left[\int_x^1 \frac{dy}{y} \frac{y A_n^+(y) - x A_n^+(x)}{y-x} + A_n^+(x) \log(1-x) \right] + \right.$$
$$\left. -2C_F \left(\int_x^1 \frac{dy}{y} A_n^+(y) \right) + C_F \frac{3}{2} A_n^+(x) \right\} - \frac{1}{4\pi\beta_0} K_1^+ A_n^+(x) + \int_x^1 \frac{dy}{y} \left[K_2^+(z) S_2(z) + \right.$$
$$\left. + K_3^+(z) \log(z) + \log^2(z) K_4^+(z) + \log(z) \log(1-z) K_5^+(z) \right] \left(-\frac{1}{4\pi\beta_0} \right) A_n^+(y) +$$
$$K_6^+ \left(-\frac{1}{4\pi\beta_0} \right) \left\{ \left[\int_x^1 \frac{dy}{y} \frac{y A_n^+(y) - x A_n^+(x)}{y-x} + A_n^+(x) \log(1-x) \right] + K_7^+ \int_x^1 \frac{dy}{y} A_n^+(y) \right\} -$$
$$C_F \left(-\frac{4}{\beta_0} \right) \left[\int_x^1 \frac{dy}{y} \frac{y B_n^{\pm}(y) - x B_n^{\pm}(x)}{y-x} + B_n^{\pm}(x) \log(1-x) \right] +$$
$$C_F \left(\frac{4}{\beta_0} \right) \left(\int_x^1 \frac{dy}{y} B_n^{\pm}(y) \right) + C_F \left(-\frac{2}{\beta_0} \right) \frac{3}{2} B_n^{\pm}(x) \,. \tag{60}$$

As we have already mentioned, the implementation of these recursion relations require particular numerical care, since, as n increases, numerical instabilities tend to add up unless high accuracy is used in the computation of the integrals. In particular we use finite element expansions to extract analitically the logarithms in the convolution (see the discussion in Appendix A). NLO plots of the coefficients $A_n(x) + \alpha(Q^2) B_n(x)$ are shown in figs. (4,5) for a specific set of initial conditions (GRSV, as discussed below). As the index n increases, the number of nodes also increases. A stable implementation can be reached for several thousands of grid-points and up to $n \approx 10$. Notice that the asymptotic expansion is suppressed by $n!$ and that additional contributions ($n > 10$) are insignificant even at large (> 200 GeV) final evolution scales Q.

7 Nonforward Extensions

In this section we finally discuss the nonforward extension of the evolution algorithm. In the case of nonforward distributions a second scaling parameter ζ controls the asymmetry between the initial and the final nucleon momentum in the deeply virtual limit of nucleon Compton scattering. The solution of the evolution equations, in this case, are known in operatorial form. Single and double parton distributions are obtained sandwiching the operatorial solution with 4 possible types of initial/final states $< p|...|p >, < p|...|0 >, < p'|...|p >$, corresponding, respectively, to the case of diagonal parton distributions, distribution amplitudes and, in the latter case, skewed and double

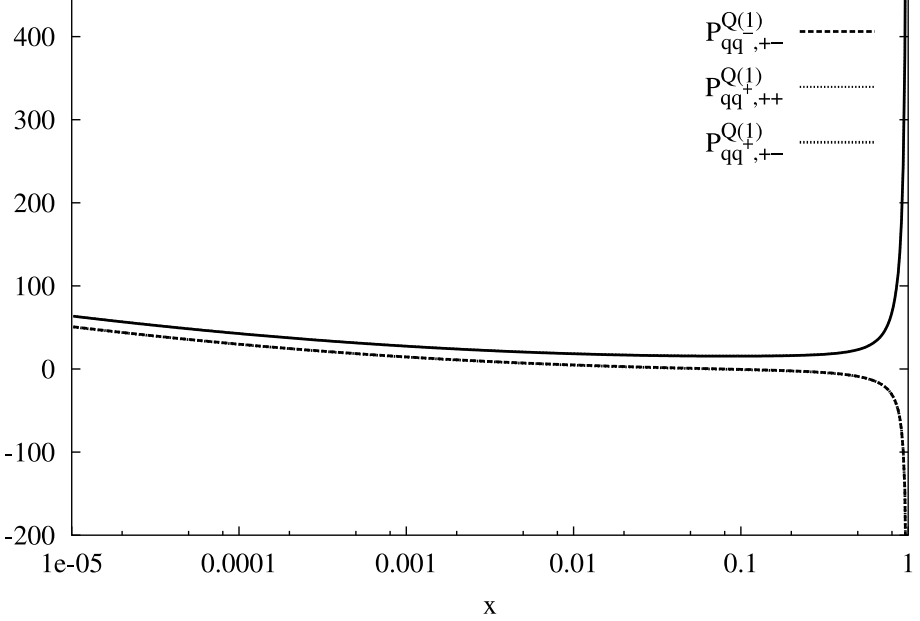

Figure 3: Plot of the NLO kernels for the **Q** distributions, showing a negative behaviour at large x

parton distributions [2]. Here we will simply analize the non-singlet case and discuss the extension of the forward algorithm to this more general case. Therefore, given the off-forward distributions $H_q(x,\xi)$, in Ji's notation, we set up the expansion

$$H_q(x,\xi) = \sum_{k=0}^{\infty} \frac{A_k(x,\xi)}{k!} \log^k\left(\frac{\alpha(Q^2)}{\alpha(Q_0^2)}\right) + \alpha(Q^2) \sum_{k=0}^{\infty} \frac{B_k(x,\xi)}{k!} \log^k\left(\frac{\alpha(Q^2)}{\alpha(Q_0^2)}\right), \tag{61}$$

which is the natural extension of the forward algorithm discussed in the previous sections. We recall that in the light-cone gauge $H(x,\xi)$ is defined as

$$H_q(x,\xi,\Delta^2)) = \frac{1}{2}\int \frac{dy^-}{2\pi} e^{-ix\bar{P}^+y^-} \langle P'|\bar{\psi}_q(0,\frac{y^-}{2},\mathbf{0}_\perp)\frac{1}{2}\gamma^+\psi_q(0,\frac{y^-}{2},\mathbf{0}_\perp)|P\rangle \tag{62}$$

with $\Delta = P' - P$, $\bar{P}^+ = 1/2(P+\bar{P})$ [1] (symmetric choice) and $\xi\bar{P} = 1/2\ \Delta^+$.

This distribution describes for $x > \xi$ and $x < -\xi$ the DGLAP-type region for the quark and the antiquark distribution respectively, and the ERBL [22] (see also [23] for an overview) distribution amplitude for $-\xi < x < \xi$. In the following we will omit the Δ dependence from H_q.

Again, once we insert the ansatz (61) into the evolution equations we obtain an infinite set of recursion relations which we can solve numerically. In LO, it is rather simple to relate the Gegenbauer moments of the skewed distributions and those of the generalized scaling coefficients A_n. We recall that in the nonforward evolution, the multiplicatively renormalizable operators appearing in the light cone expansion are given in terms of Gegenbauer polynomials [2]. The Gegenbauer moments of the coefficients A_n of our expansion (61) can be easily related to those of the off-forward distribution

$$C_n(\xi,Q^2) = \zeta^n \int_{-1}^{1} C_n^{3/2}(z/\xi) H(z,\xi,Q^2) dz. \tag{63}$$

The evolution of these moments is rather simple

$$C_n(\zeta,Q^2) = C_n(\zeta,Q_0^2)\left(\frac{\alpha(Q^2)}{\alpha(Q_0^2)}\right)^{\gamma_n/\beta_0} \tag{64}$$

$$\gamma_n = C_F \left(\frac{1}{2} - \frac{1}{(n+1)(n+2)} + 2 \sum_{j=2} \frac{1}{j} \right) \tag{65}$$

being the non-singlet anomalous dimensions. If we define the Gegenbauer moments of our expansion

$$A_k^{(n)}(\xi, Q^2) = \xi^n \int_{-1}^{1} C_n^{3/2}(z/\xi) H(z\,\xi, Q^2) dz \tag{66}$$

we can relate the moments of the two expansions as

$$A_k^{(n)}(\xi) = C_n(\zeta, Q_0^2) \left(\frac{\gamma_n}{\beta_0} \right)^k . \tag{67}$$

Notice that expansions similar to (61) hold also for other choices of kinematical variables, such as those defining the non-forward distributions [2], where the t-channel longitudinal momentum exchange Δ^+ is related to the longitudinal momentum of the incoming nucleon as $\Delta = \zeta P$. We recall that $H_q(x.\xi)$ as defined in [1] can be mapped into two independent distributions $\hat{\mathcal{F}}_q(X,\zeta)$ and $\hat{\mathcal{F}}_{\bar{q}}(X,\zeta)$ through the mappings [16]

$$\begin{aligned} X_1 &= \frac{(x_1+\xi)}{(1+\xi)} \\ X_2 &= \frac{\xi - x_2}{(1+\xi)} \\ \xi &= \zeta/(2-\zeta) \\ \mathcal{F}_q(X_1,\zeta) &= \frac{1}{1-\zeta/2} H_q(x_1,\xi) \\ \mathcal{F}_{\bar{q}}(X_2,\zeta) &= \frac{-1}{1-\zeta/2} H_q(x_2,\xi), \end{aligned} \tag{68}$$

in which the interval $-1 \le x \le 1$ is split into two coverings, partially overlapping (for $-\xi \le x \le \xi$, or ERBL region) in terms of the two variables $-\xi \le x_1 \le 1$ ($0 \le X_1 \le 1$) and $-1 \le x_2 \le \xi$ ($0 \le X_2 \le 1$). In this new parameterization, the momentum fraction carried by the emitted quark is X, as in the case of ordinary distributions, where it is parametrized by Bjorken x. For definitess, we focus here on the DGLAP-like ($X > \zeta$) region of the non-singlet evolution. The non-singlet kernel is given in this case by ($x \equiv X$)

$$P_\zeta(x,\zeta) = \frac{\alpha}{\pi} C_F \left(\frac{1}{y-x} \left[1 + \frac{xx'}{yy'} \right] - \delta(x-y) \int_0^1 dz \frac{1+z^2}{1-z} \right), \tag{69}$$

we introduce a LO ansatz

$$\mathcal{F}_q(x,\zeta) = \sum_{k=0}^{\infty} \frac{\mathcal{A}_k(x,\zeta)}{k!} \log^k \left(\frac{\alpha(Q^2)}{\alpha(Q_0^2)} \right) \tag{70}$$

and insert it into the evolution of this region to obtain the very simple recursion relations

$$\begin{aligned} \mathcal{A}_{n+1}(X,\zeta) &= -\frac{2}{\beta_0} C_F \int_X^1 \frac{dy}{y} \frac{y\mathcal{A}_n(y,\zeta) - x\mathcal{A}_n(X,\zeta)}{y-X} - \frac{2}{\beta_0} C_F \int_X^1 \frac{dy(X-\zeta)}{y(y-\zeta)} \frac{(y\mathcal{A}_n(X,\zeta) - X\mathcal{A}_n(y,\zeta))}{y-X} \\ &\quad -\frac{2}{\beta_0} C_F \hat{\mathcal{A}}_n(X,\zeta) \left[\frac{3}{2} + \ln \frac{(1-X)^2(1-x/\zeta)}{1-\zeta} \right]. \end{aligned} \tag{71}$$

The recursion relations can be easily reduced to a weighted sum of contributions in which ζ is a spectator parameter. Here we will not make a complete implementation, but we will illustrate in an appendix the general strategy to be followed. There we show a very accurate analytical method to evaluate the logarithms generated by the expansion without having to rely on brute-force computations.

Positivity of the non-singlet evolution is a simple consequence of the master-form associated to the non-forward kernel (69). As we have already emphasized above, positivity of the initial conditions are sufficient to guarantee a positivity of the solution at any scale Q. The master-form of the equation allows to reinterpret the parton dynamics as a random walk biased toward small-x values as $\tau = \log(Q^2)$ increases.

In the non-forward case the identification of a transition probability for the random walk [6] associated with the evolution of the parton distribution is obtained via the non-forward transition probability

$$\begin{aligned} w_\zeta(x|y) &= \frac{\alpha}{\pi} C_F \frac{1}{y-x}\left[1+\frac{x}{y}\frac{(x-\zeta)}{y-\zeta}\right]\theta(y>x) \\ w'_\zeta(y|x) &= \frac{\alpha}{\pi} C_F \frac{x^2+y^2}{x^2(x-y)}\theta(y<x) \end{aligned} \tag{72}$$

and the corresponding master equation is given by

$$\frac{d\mathcal{F}_q}{d\tau} = \int_x^1 dy\, w_\zeta(x|y)\mathcal{F}_q(y,\zeta,\tau) - \int_0^x dy\, w'_\zeta(y|x)\mathcal{F}_q(x,\zeta,\tau), \tag{73}$$

that can be re-expressed in a form which is a simple generalization of the formula for the forward evolution [6]

$$\begin{aligned} \frac{d\mathcal{F}_q}{d\log Q^2} &= \int_x^1 dy\, w_\zeta(x|y)\mathcal{F}_q(y,\zeta,\tau) - \int_0^x dy\, w'_\zeta(y|x)\mathcal{F}_q(x,\zeta,\tau) \\ &= -\int_0^{\alpha(x)} dy w_\zeta(x+y|x) * \mathcal{F}_q(x,\zeta,\tau) + \int_0^{-x} dy\, w'_\zeta(x+y|x)\mathcal{F}_q(x,\zeta,\tau), \end{aligned} \tag{74}$$

where a Moyal-like product appears

$$w_\zeta(x+y|x) * \mathcal{F}_q(x,\zeta,\tau) \equiv w_\zeta(x+y|x) e^{-y\left(\overleftarrow{\partial}_x + \overrightarrow{\partial}_x\right)} \mathcal{F}_q(x,\zeta,\tau) \tag{75}$$

and $\alpha(x) = x - 1$. A Kramers-Moyal expansion of the equation allows to generate a differential equation of infinite order with a parametric dependence on ζ

$$\begin{aligned} \frac{d\mathcal{F}_q}{d\log Q^2} &= \int_{\alpha(x)}^0 dy\, w_\zeta(x+y|x)\mathcal{F}_q(x,\zeta,\tau) + \int_0^{-x} dy\, w'_\zeta(x+y|x)\mathcal{F}_q(x,\zeta,\tau) \\ &\quad - \sum_{n=1}^{\infty} \int_0^{\alpha(x)} dy \frac{(-y)^n}{n!} \partial_x{}^n \left(w_\zeta(x+y|x)\mathcal{F}_q(x,\zeta,\tau)\right). \end{aligned} \tag{76}$$

We define

$$\begin{aligned} \tilde{a}_0(x,\zeta) &= \int_{\alpha(x)}^0 dy w_\zeta(x+y|x)\mathcal{F}_q(x,\zeta,\tau) + \int_0^{-x} dy\, w'_\zeta(x+y|x)\mathcal{F}_q(x,\zeta,\tau) \\ a_n(x,\zeta) &= \int_0^{\alpha(x)} dy\, y^n w_\zeta(x+y|x)\mathcal{F}_q(x,\zeta,\tau) \\ \tilde{a}_n(x,\zeta) &= \int_0^{\alpha(x)} dy y^n \partial_x{}^n \left(w_\zeta(x+y|x)\mathcal{F}_q(x,\zeta,\tau)\right) \quad n=1,2,... \end{aligned} \tag{77}$$

If we arrest the expansion at the first two terms ($n = 1, 2$) we are able to derive an approximate equation describing the dynamics of partons for non-diagonal transitions. The procedure is a

purpose we use the identities

$$\begin{aligned}
\tilde{a}_1(x,\zeta) &= \partial_x a_1(x,\zeta) - \alpha(x)\partial_x\alpha(x) w_\zeta(x+\alpha(x)|x)\mathcal{F}_q(x,\zeta,\tau) \\
\tilde{a}_2(x,\zeta) &= \partial_x^2 a_2(x,\zeta) - 2\alpha(x)(\partial_x\alpha(x))^2 w_\zeta(x+\alpha(x)|x)\mathcal{F}_q(x,\zeta,\tau) \\
&\quad -\alpha(x)^2\partial_x\alpha(x)\partial_x\left(w_\zeta(x+\alpha(x)|x)\mathcal{F}_q(x,\zeta,\tau)\right) \\
&\quad -\alpha^2(x)\partial_x\alpha(x)\partial_x\left(w_\zeta(x+y|x)\mathcal{F}_q(x,\zeta,\tau)\right)|_{y=\alpha(x)}.
\end{aligned} \tag{78}$$

which allow to compute the first few coefficients of the expansion. Using these relations, the Fokker-Planck approximation to this equation can be worked out explicitely. We omit details on the derivation which is unobvious since particular care is needed to regulate the (canceling) divergences and just quote the result.

A lengthy computation gives

$$\begin{aligned}
\frac{d\mathcal{F}_q}{d\tau} &= \frac{\alpha}{\pi}C_F\left(\frac{x_{0,-3}}{(x-\zeta)^3}+\frac{x_{0,-1}}{(x-\zeta)}+x_{0,0}\right)\mathcal{F}_q(x,\zeta,\tau) \\
&\quad +\frac{\alpha}{\pi}C_F\left(\frac{x_{1,-3}}{(x-\zeta)^3}+\frac{x_{1,-1}}{(x-\zeta)}\right)\partial_x\mathcal{F}_q(x,\zeta,\tau)+\frac{\alpha}{\pi}C_F\frac{x_{0,-3}}{(x-\zeta)^3}\partial_x^2\mathcal{F}_q(x,\zeta,\tau)
\end{aligned} \tag{79}$$

where we have defined

$$\begin{aligned}
x_{0,-3} &= \frac{-\left((-1+x)^3\,(17x^3-\zeta^2(3+4\zeta)+3x\zeta(3+5\zeta)-3x^2(3+7\zeta))\right)}{12\,x^3} \\
x_{0,-1} &= \frac{-29x^4-3+x^2\,(-1+\zeta)+2\zeta-2x(1+3\zeta)+x^3(12+23\zeta)}{3x^3} \\
x_{0,0} &= 4+\frac{1}{2x^2}-\frac{3}{x}+2\log\frac{(1-x)}{x} \\
x_{1,-1} &= \frac{-\left((-1+6x-15x^2+14x^3)\,(x-\zeta)\right)}{3x^2} \\
x_{1,-3} &= \frac{1}{2}-\frac{5x}{3}+5x^3-\frac{23x^4}{6}+\frac{7\zeta}{3}-\frac{3\zeta}{4x}+\frac{5x\zeta}{2} \\
&\quad -15x^2\zeta+\frac{131x^3\zeta}{12}-\frac{5\zeta^2}{2}+\frac{\zeta^2}{4x^2}-\frac{\zeta^2}{x}+13x\zeta^2-\frac{39x^2\zeta^2}{4}-3\zeta^3+\frac{\zeta^3}{3x^2}+\frac{8x\zeta^3}{3} \\
x_{2,-3} &= \frac{-\left((-1+x)^2(x-\zeta)^2\,(3+23x^2+4\zeta-2x(7+8\zeta))\right)}{24x}.
\end{aligned} \tag{80}$$

This equation and all the equations obtained by arresting the Kramers-Moyal expansion to higher order provide a complementary description of the non-forward dynamics in the DGLAP region, at least in the non-singlet case. Moving to higher order is straightforward although the results are slightly lengthier. A full-fledged study of these equations is under way and we expect that the DGLAP dynamics is reobtained - directly from these equations - as the order of the approximation increases.

9 Model Comparisons, Saturation and the Tensor Charge

In this last section we discuss some implementations of our methods to the standard (forward) evolution by doing a NLO model comparisons both in the analysis of Soffer's inequality and for the evolution of the tensor charge. We have selected two models, motivated quite independently and we have compared the predicted evolution of the Soffer bound at an accessable final evolution

this point we recall that in order to generate suitable initial conditions for the analysis of Soffer's inequality, one needs an ansatz in order to quantify the difference between its left-hand side and right-hand side at its initial value.

The well known strategy to build reasonable initial conditions for the transverse spin distribution consists in generating polarized distributions (starting from the unpolarized ones) and then saturate the inequality at some lowest scale, which is the approach we have followed for all the models that we have implemented.

Following Ref. [18] (GRSV model), we have used as input distributions - in the unpolarized case - the formulas in Ref. [17], calculated to NLO in the $\overline{\rm MS}$ scheme at a scale $Q_0^2 = 0.40\,{\rm GeV}^2$

$$\begin{aligned}
x(u-\overline{u})(x,Q_0^2) &= 0.632x^{0.43}(1-x)^{3.09}(1+18.2x) \\
x(d-\overline{d})(x,Q_0^2) &= 0.624(1-x)^{1.0}x(u-\overline{u})(x,Q_0^2) \\
x(\overline{d}-\overline{u})(x,Q_0^2) &= 0.20x^{0.43}(1-x)^{12.4}(1-13.3\sqrt{x}+60.0x) \\
x(\overline{u}+\overline{d})(x,Q_0^2) &= 1.24x^{0.20}(1-x)^{8.5}(1-2.3\sqrt{x}+5.7x) \\
xg(x,Q_0^2) &= 20.80x^{1.6}(1-x)^{4.1}
\end{aligned} \tag{81}$$

and $xq_i(x,Q_0^2) = x\overline{q_i}(x,Q_0^2) = 0$ for $q_i = s,c,b,t$.

We have then related the unpolarized input distribution to the longitudinally polarized ones by as in Ref. [18]

$$\begin{aligned}
x\Delta u(x,Q_0^2) &= 1.019x^{0.52}(1-x)^{0.12}xu(x,Q_0^2) \\
x\Delta d(x,Q_0^2) &= -0.669x^{0.43}xd(x,Q_0^2) \\
x\Delta\overline{u}(x,Q_0^2) &= -0.272x^{0.38}x\overline{u}(x,Q_0^2) \\
x\Delta\overline{d}(x,Q_0^2) &= x\Delta\overline{u}(x,Q_0^2) \\
x\Delta g(x,Q_0^2) &= 1.419x^{1.43}(1-x)^{0.15}xg(x,Q_0^2)
\end{aligned} \tag{82}$$

and $x\Delta q_i(x,Q_0^2) = x\Delta\overline{q_i}(x,Q_0^2) = 0$ for $q_i = s,c,b,t$.

Following [21], we assume the saturation of Soffer inequality:

$$x\Delta_T q_i(x,Q_0^2) = \frac{xq_i(x,Q_0^2) + x\Delta q_i(x,Q_0^2)}{2} \tag{83}$$

and study the impact of the different evolutions on both sides of Soffer's inequality at various final evolution scales Q.

In the implementation of the second model (GGR model) we have used as input distributions in the unpolarized case the CTEQ4 parametrization [19], calculated to NLO in the $\overline{\rm MS}$ scheme at a scale $Q_0 = 1.0\,{\rm GeV}$

$$\begin{aligned}
x(u-\overline{u})(x,Q_0^2) &= 1.344x^{0.501}(1-x)^{3.689}(1+6.402x^{0.873}) \\
x(d-\overline{d})(x,Q_0^2) &= 0.64x^{0.501}(1-x)^{4.247}(1+2.69x^{0.333}) \\
xs(x,Q_0^2) = x\overline{s}(x,Q_0^2) &= 0.064x^{-0.143}(1-x)^{8.041}(1+6.112x) \\
x(\overline{d}-\overline{u})(x,Q_0^2) &= 0.071x^{0.501}(1-x)^{8.041}(1+30.0x) \\
x(\overline{u}+\overline{d})(x,Q_0^2) &= 0.255x^{-0.143}(1-x)^{8.041}(1+6.112x) \\
xg(x,Q_0^2) &= 1.123x^{-0.206}(1-x)^{4.673}(1+4.269x^{1.508})
\end{aligned} \tag{84}$$

and $xq_i(x,Q_0^2) = x\overline{q_i}(x,Q_0^2) = 0$ for $q_i = c,b,t$ and we have related the unpolarized input distribution to the longitudinally polarized ones by the relations [20]

$$
\begin{aligned}
x\Delta\overline{u}(x,Q_0^2) &= x\eta_u(x)xu(x,Q_0^2) \\
x\Delta u(x,Q_0^2) &= \cos\theta_D(x,Q_0^2)\left[x(u-\overline{u})-\frac{2}{3}x(d-\overline{d})\right](x,Q_0^2)+x\Delta\overline{u}(x,Q_0^2) \\
x\Delta\overline{d}(x,Q_0^2) &= x\eta_d(x)xd(x,Q_0^2) \\
x\Delta d(x,Q_0^2) &= \cos\theta_D(x,Q_0^2)\left[-\frac{1}{3}x(d-\overline{d})(x,Q_0^2)\right]+x\Delta\overline{d}(x,Q_0^2) \\
x\Delta s(x,Q_0^2)=x\Delta\overline{s}(x,Q_0^2) &= x\eta_s(x)xs(x,Q_0^2)
\end{aligned}
\tag{85}
$$

and $x\Delta q_i(x,Q_0^2)=x\Delta\overline{q_i}(x,Q_0^2)=0$ for $q_i=c,b,t$.

A so-called "spin dilution factor" as defined in [20], which appears in the equations above is given by

$$
\cos\theta_D(x,Q_0^2)=\left[1+\frac{2\alpha_s(Q^2)}{3}\frac{(1-x)^2}{\sqrt{x}}\right]^{-1}. \tag{86}
$$

In this second (GGR) model, in regard to the initial conditions for the gluons, we have made use of two different options, characterized by a parameter η dependent on the corresponding option. The first option, that we will denote by GGR1, assumes that gluons are moderately polarized

$$
\begin{aligned}
x\Delta g(x,Q_0^2) &= x\cdot xg(x,Q_0^2) \\
\eta_u(x)=\eta_d(x) &= -2.49+2.8\sqrt{x} \\
\eta_s(x) &= -1.67+2.1\sqrt{x},
\end{aligned}
\tag{87}
$$

while the second option (GGR2) assumes that gluons are not polarized

$$
\begin{aligned}
x\Delta g(x,Q_0^2) &= 0 \\
\eta_u(x)=\eta_d(x) &= -3.03+3.0\sqrt{x} \\
\eta_s(x) &= -2.71+2.9\sqrt{x}.
\end{aligned}
\tag{88}
$$

We have plotted both ratios Δ_T/f^+ and differences $(xf^+-x\Delta_T f)$ for various flavours as a function of x. For the up quark, while the two models GGR1 and GGR2 are practically overlapping, the difference between the GGR and the GRSV models in the the ratio $\Delta_T u/u^+$ is only slightly remarked in the intermediate x region $(0.1-0.5)$. In any case, it is just at the few percent level (Fig. (6)), while the inequality is satisfied with a ratio between the plus helicity distribution and transverse around 10 percent from the saturation value, and above. There is a wider gap in the inequality at small x, region characterized by larger transverse distribution, with values up to 40 percent from saturation. A similar trend is noticed for the x-behaviour of the inequality in the case of the down quark (Fig. 7). In this latter case the GGR and the GRSV model show a more remarked difference, especially for intermediate x-values. An interesting features appears in the corresponding plot for the strange quark (Fig.(8)), showing a much wider gap in the inequality (50 percent and higher) compared to the other quarks. Here we have plotted results for the two GGR models (GGR1 and GGR2). Differently from the case of the other quarks, in this case we observe a wider gap between lhs and rhs at larger x values, increasing as $x\to 1$. In figs. (9)and (10) we plot the differences $(xf^+-x\Delta_T f)$ for strange and charm and for bottom and top quarks respectively, which show a much more reduced evolution from the saturation value up to the final corresponding evolving scales (100 and 200 GeV). As a final application we finally discuss the behaviour of the tensor charge of the up quark for the two models as a function of the final evolution scale Q. We recall that like the isoscalar and the isovector axial vector charges defined from the forward matrix element of the nucleon, the nucleon tensor charge is defined from the matrix element of the tensor current

$$
\langle PS_T|\bar{\psi}\sigma^{\mu\nu}\gamma_5\lambda^a\psi|P,S_T\rangle=2\delta q^a(Q_0^2)\,(P^\mu S_T^\nu-P^\nu S_T^\mu) \tag{89}
$$

S_T is the transverse spin.

In fig. (11) we plot the evolution of the tensor charge for the models we have taken in exam. At the lowest evolution scales the charge is, in these models, above 1 and decreases slightly as the factorization scale Q increases. We have performed an evolution up to 200 GeV as an illustration of this behaviour. There are substantial differences between these models, as one can easily observe, which are around 20 percent. From the analysis of these differences at various factorization scales we can connect low energy dynamics to observables at higher energy, thereby distinguishing between the various models. Inclusion of the correct evolution, up to subleading order is, in general, essential.

10 Conclusions

We have illustrated the use of x-space based algorithms for the solution of evolution equations in the leading and in the next-to-leading approximation and we have provided some applications of the method both in the analysis of Soffer's inequality and in the investigation of other relations, such as the evolution of the proton tensor charge, for various models. The evolution has been implemented using a suitable base, relevant for an analysis of positivity in LO, using kinetic arguments. The same kinetic argument has been used to prove the positivity of the evolution of h_1 and of the tensor charge up to NLO. In our implementations we have completely relied on recursion relations without any reference to Mellin moments. We have provided several illustrations of the recursive algorithm and extended it to the non-forward evolution up to NLO. Building on previous work for the forward evolution, we have presented a master-form of the non-singlet evolution of the skewed distributions, a simple proof of positivity and a related Kramers Moyal expansion, valid in the DGLAP region of the skewed evolution for any value of the asymmetry parameter ζ. We hope to return with a complete study of the nonforward evolution and related issues not discussed here in the near future.

Acknowledgements

C.C. thanks Prof. Ph. Jetzer and the Theory Group at the University of Zurich for hospitality while completing this work.

11 Appendix A. Weighted Sums

In this appendix we briefly illustrate the reduction of recursion relations to analytic expressions based on finite element decompositions of the corresponding integrals. The method allows to write in analytic forms the most dangerous integrals thereby eliminating possible sources of instabilities in the implementation of the recursion relations. The method uses a linear interpolation formula for the coefficients A_n, B_n which, in principle can also be extended to higher (quadratic) order. However, enugh accuracy can be achieved by increasing the grid points in the discretization. Notice that using this method we can reach any accuracy since we have closed formulas for the integrals. In practice these and similar equations are introduced analytically as functions in the numerical integration procedures.

Below, we will use a simplified notation ($X \equiv x$ for simplicity).

We define $\bar{P}(x,\zeta) \equiv xP(x,\zeta)$ and $\bar{A}(x,\zeta) \equiv xA(x)$ and the convolution products

$$J(x) \equiv \int_x^1 \frac{dy}{y} \left(\frac{x}{y}\right) P\left(\frac{x}{y},\zeta\right) \bar{A}(y). \tag{90}$$

ordered from left to right $(x_0, x_1, x_2, ..., x_n, x_{n+1})$ with $x_0 = x$ and $x_{n+1} = 1$ being the upper edge of the integration region. One constructs a rescaled array $(x, x/x_n, ..., x/x_2, x/x_1, 1)$. We define $s_i \equiv x/x_i$, and $s_{n+1} = x < s_n < s_{n-1} < ...s_1 < s_0 = 1$. We get

$$J(x,\zeta) = \sum_{i=0}^{N} \int_{x_i}^{x_{i+1}} \frac{dy}{y} \left(\frac{x}{y}\right) P\left(\frac{x}{y}, \zeta\right) \bar{A}(y,\zeta) \tag{91}$$

At this point we introduce the linear interpolation

$$\bar{A}(y,\zeta) = \left(1 - \frac{y - x_i}{x_{i+1} - x_i}\right) \bar{A}(x_i,\zeta) + \frac{y - x_i}{x_{i+1} - x_i} \bar{A,}\zeta(x_{i+1}) \tag{92}$$

and perform the integration on each subinterval with a change of variable $y- > x/y$ and replace the integral $J(x,\zeta)$ with its discrete approximation $J_N(x)$ to get

$$\begin{aligned} J_N(x,\zeta) &= \bar{A}(x_0)\frac{1}{1-s_1}\int_{s_1}^{1}\frac{dy}{y}P(y,\zeta)(y-s_1) \\ &+ \sum_{i=1}^{N}\bar{A}(x_i,\zeta)\frac{s_i}{s_i - s_{i+1}}\int_{s_{i+1}}^{s_i}\frac{dy}{y}P(y)(y-s_{i+1}) \\ &- \sum_{i=1}^{N}\bar{A}(x_i,\zeta)\frac{s_i}{s_{i-1} - s_i}\int_{s_i}^{s_{i-1}}\frac{dy}{y}P(y,\zeta)(y-s_{i-1}) \end{aligned} \tag{93}$$

with the condition $\bar{A}(x_{N+1},\zeta) = 0$. Introducing the coefficients $W(x,x,\zeta)$ and $W(x_i,x,\zeta)$, the integral is cast in the form

$$J_N(x,\zeta) = W(x,x,\zeta)\bar{A}(x,\zeta) + \sum_{i=1}^{n} W(x_i,x,\zeta)\bar{A}(x_i,\zeta) \tag{94}$$

where

$$\begin{aligned} W(x,x,\zeta) &= \frac{1}{1-s_1}\int_{s_1}^{1}\frac{dy}{y}(y-s_1)P(y,\zeta), \\ W(x_i,x,\zeta) &= \frac{s_i}{s_i - s_{i+1}}\int_{s_{i+1}}^{s_i}\frac{dy}{y}\left(y-s_{i+1}\right)P(y,\zeta) \\ &- \frac{s_i}{s_{i-1} - s_i}\int_{s_i}^{s_{i-1}}\frac{dy}{y}\left(y-s_{i-1}\right)P(y,\zeta). \end{aligned} \tag{95}$$

For instance, after some manipulations we get

$$\int_X^1 \frac{dy}{y}\frac{y\mathcal{A}_n(y,\zeta) - x\mathcal{A}_n(X,\zeta)}{y-X} = \mathbf{In_0}(x)\mathcal{A}_n(x,\zeta) + \sum_{i+1}^{N}\left(\mathbf{Jn_i}(x) - \mathbf{Jnt_i}(x)\right)\mathcal{A}_n(x_i) - \ln(1-x)\mathcal{A}_n(x,\zeta) \tag{96}$$

where

$$\begin{aligned} \mathbf{I_0}(x) &= \frac{1}{1-s_1}\log(s_1) + \log(1-s_1) \\ \mathbf{J_i}(x) &= \frac{1}{s_i - s_{i+1}}\left[\log\left(\frac{1-s_{i+1}}{1-s_i}\right) + s_{i+1}\log\left(\frac{1-s_i}{1-s_{i+1}}\frac{s_{i+1}}{s_i}\right)\right] \\ \mathbf{J'_i}(x) &= \frac{1}{s_{i-1} - s_i}\left[\log\left(\frac{1-s_i}{1-s_{i-1}}\right) + s_{i-1}\log\left(\frac{s_i}{s_{i-1}}\right) + s_{i-1}\left(\frac{1-s_{i-1}}{1-s_i}\right)\right], \quad i = 2,3,..N \\ \mathbf{J_1}(x) &= \frac{1}{1-s_1}\log s_1. \end{aligned} \tag{97}$$

allow to obtain very fast and extremely accurate implementations for any ζ.

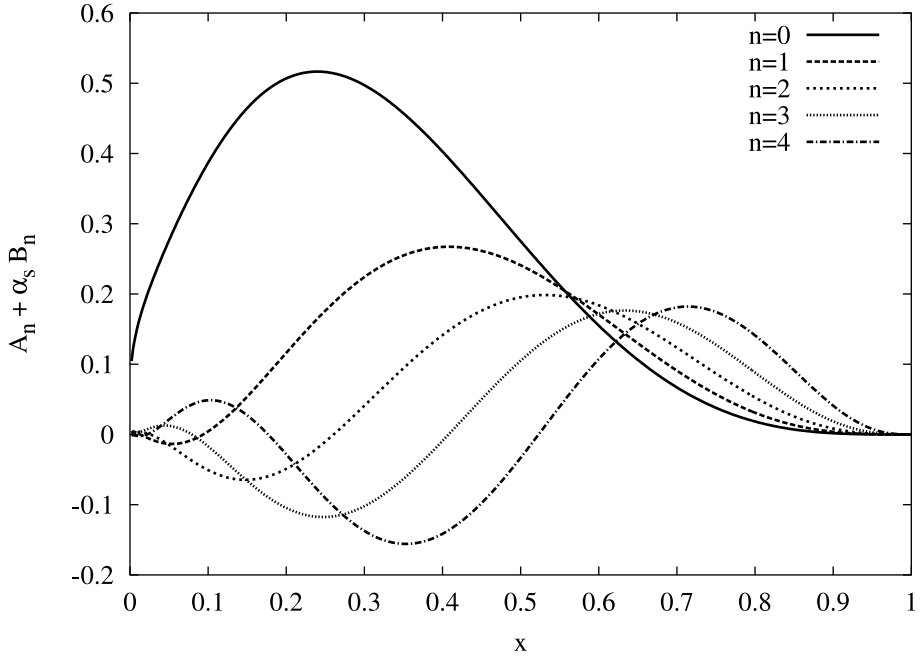

Figure 4: Coefficients $A_n(x) + \alpha_s(Q^2)B_n$, with $n = 0, \ldots, 4$ for a final scale $Q = 100$ GeV for the quark up.

12 Appendix B

n_f	A	B
3	12.5302	12.1739
4	10.9569	10.6924
5	9.3836	9.2109
6	7.8103	7.7249

Table 1. Coefficients A and B for various flavour, to NLO for $\Delta_T P_{qq,\pm}$.

13 APPENDIX C

Here we define some notations in regard to the recursion relations used for the NLO evolution of the transverse spin distributions.

For the (+) case we have these expressions

$$K_1^+(x) = \frac{1}{72} C_F(-2n_f(3+4\pi^2) + N_C(51 + 44\pi^2 - 216\zeta(3)) + 9C_F(3 - 4\pi^2 + 48\zeta(3))$$

$$K_2^+(x) = \frac{2C_F(-2C_F + N_C)x}{1+x} \tag{98}$$

$$K_3^+(x) = \frac{C_F(9C_F - 11N_C + 2n_f)x}{3(x-1)} \tag{99}$$

$$K_4^+(x) = \frac{C_F N_C x}{1-x} \tag{100}$$

$$K_5^+(x) = \frac{4C_F^2 x}{1-x} \tag{101}$$

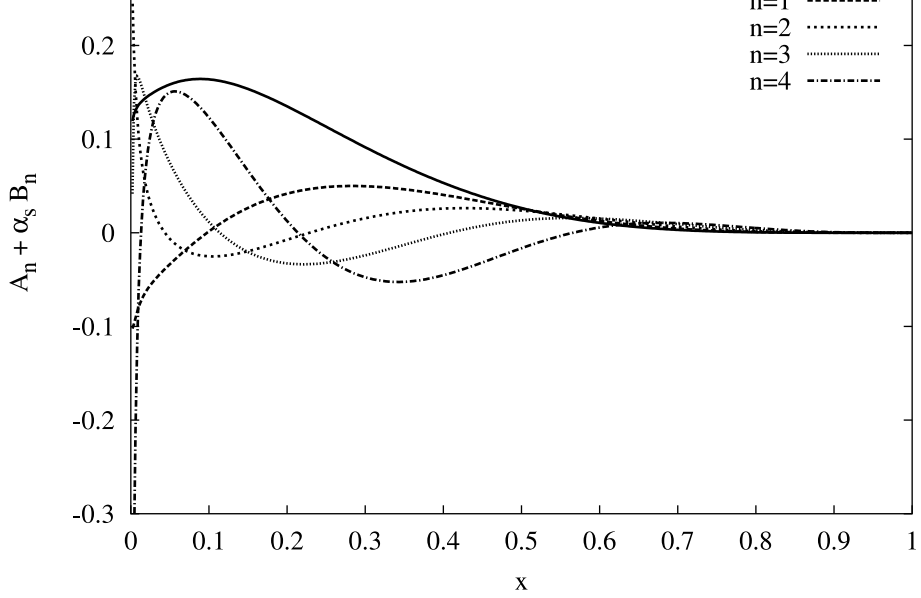

Figure 5: Coefficients $A_n(x) + \alpha_s(Q^2)B_n$, with $n = 0, \ldots, 4$ for a final scale $Q = 100$ GeV for the quark down.

$$K_6^+(x) = -\frac{1}{9}C_F(10n_f + N_C(-67 + 3\pi^2)) \tag{102}$$

$$K_7^+(x) = \frac{1}{9}C_F(10n_f + N_C(-67 + 3\pi^2)) \tag{103}$$

$$\tag{104}$$

and for the $(-)$ case we have

$$K_1^-(x) = \frac{1}{72}C_F(-2n_f(3 + 4\pi^2) + N_C(51 + 44\pi^2 - 216\zeta(3)) + 9C_F(3 - 4\pi^2 + 48\zeta(3))$$

$$K_2^-(x) = \frac{2C_F(+2C_F - N_C)x}{1 + x} \tag{105}$$

$$K_3^-(x) = \frac{C_F(9C_F - 11N_C + 2n_f)x}{3(x - 1)} \tag{106}$$

$$K_4^-(x) = \frac{C_F N_C x}{1 - x} \tag{107}$$

$$K_5^-(x) = \frac{4C_F^2 x}{1 - x} \tag{108}$$

$$K_6^-(x) = -\frac{1}{9}C_F(10n_f + N_C(-67 + 3\pi^2)) \tag{109}$$

$$K_7^-(x) = -\frac{1}{9}C_F(10n_f - 18C_F(x - 1) + N_C(-76 + 3\pi^2 + 9x)) \tag{110}$$

$$\tag{111}$$

References

[1] X. Ji, Phys.Rev.D55 (1997) 7114.

[2] A.V. Radyushkin, Phys.Rev.D56 (1997) 5524.

[3] C. Bourrely, J. Soffer, and O.V. Teryaev Phys.Lett.B420 (1998) 375.

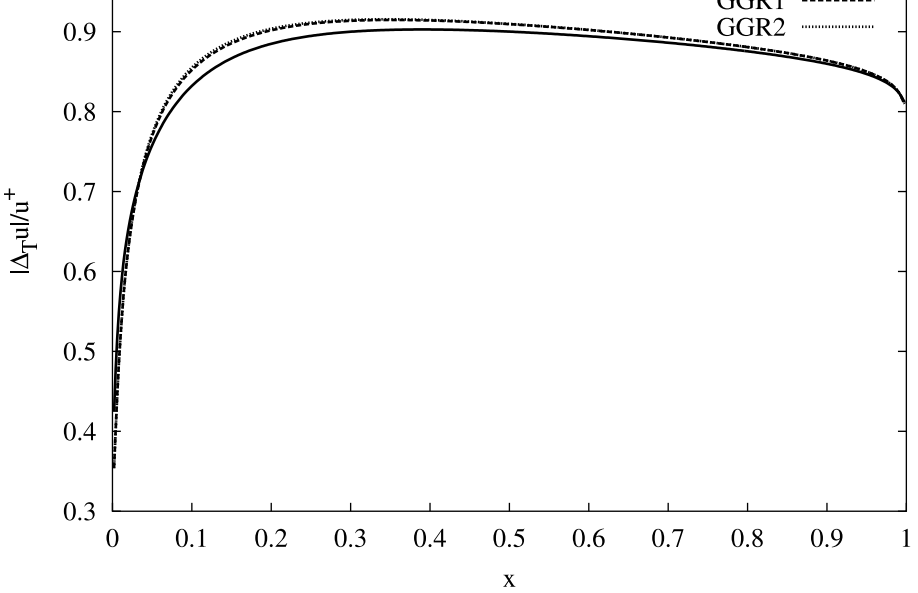

Figure 6: Test of Soffer's inequality for quark up at $Q = 100$ GeV for different models.

[4] C. Bourrely, E. Leader, O.V. Teryaev, hep-ph/9803238.

[5] R.L. Jaffe and X. Ji, Phys. Rev. Lett. 67 (1991) 552.

[6] A. Cafarella and C. Corianò, hep-ph/0301103.

[7] E. Barone, Phys.Lett.B409 (1997) 499.

[8] L.E. Gordon and G. P. Ramsey, Phys.Rev.D59 (1999) 074018.

[9] C. Corianò, Nucl.Phys.B627:66,2002.

[10] J.C. Collins and J. Qiu, Phys.Rev.D39 (1989) 1398.

[11] C. Bourrely, J. Soffer, O.V. Teryaev, Phys.Lett.B420 (1998) 375.

[12] M.Glück, E.Reya and A.Vogt, Eur.Phys.J.C 5 (1998) 461

[13] M.Glück et al., Phys.Rev.D 63 (2001) 094005

[14] O.Martin et al., Phys.Rev.D 57 (1998)

[15] G. Rossi, Phys.Rev.D29 (1984) 852.

[16] K.J. Golec-Biernat and A. D. Martin, Phys.Rev.D59 (1999) 014029.

[17] M.Glück, E.Reya and A.Vogt, Eur.Phys.J.C 5 (1998) 461

[18] M.Glück, E.Reya, M.Stratmann and W.Vogelsang, Phys.Rev.D 63 (2001) 094005

[19] H.L.Lai *et al.*, Phys.Rev.D 55 (1997) 1280.

[20] L.E.Gordon, M.Goshtasbpour and G.P.Ramsey, Phys.Rev.D 58 (1998) 094017.

[21] O.Martin, A.Schäfer, M.Stratmann and W.Vogelsang, Phys.Rev.D 57 (1998) 117502.

[22] A.V. Efremov and A.V. Radyushkin, Phys. Lett. B94 (1980) 245; G. P. Lepage and S.J. Brodsky, Phys. Rev. D22 (1980) 2157;

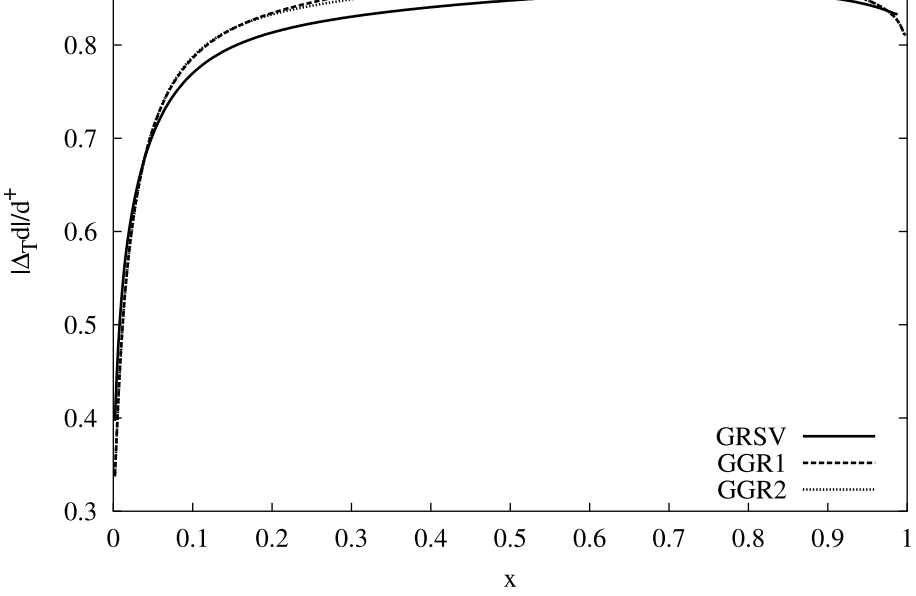

Figure 7: Test of Soffer's inequality for quark down at $Q = 100$ GeV for different models

[23] C. Corianò and H. N. Li, JHEP 9807 (1998) 008.

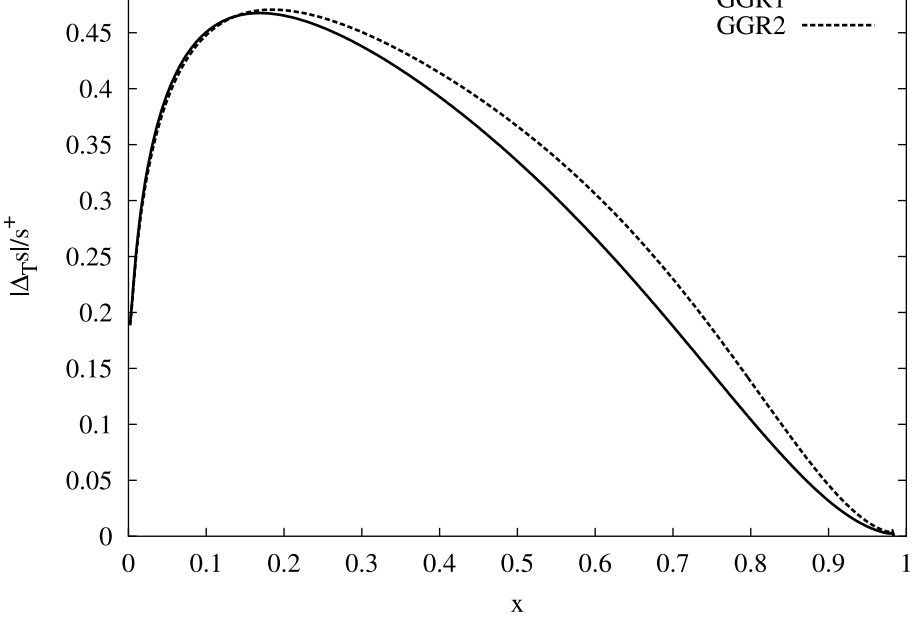

Figure 8: Test od Soffer's inequality for quark strange at $Q = 100$ GeV for different models

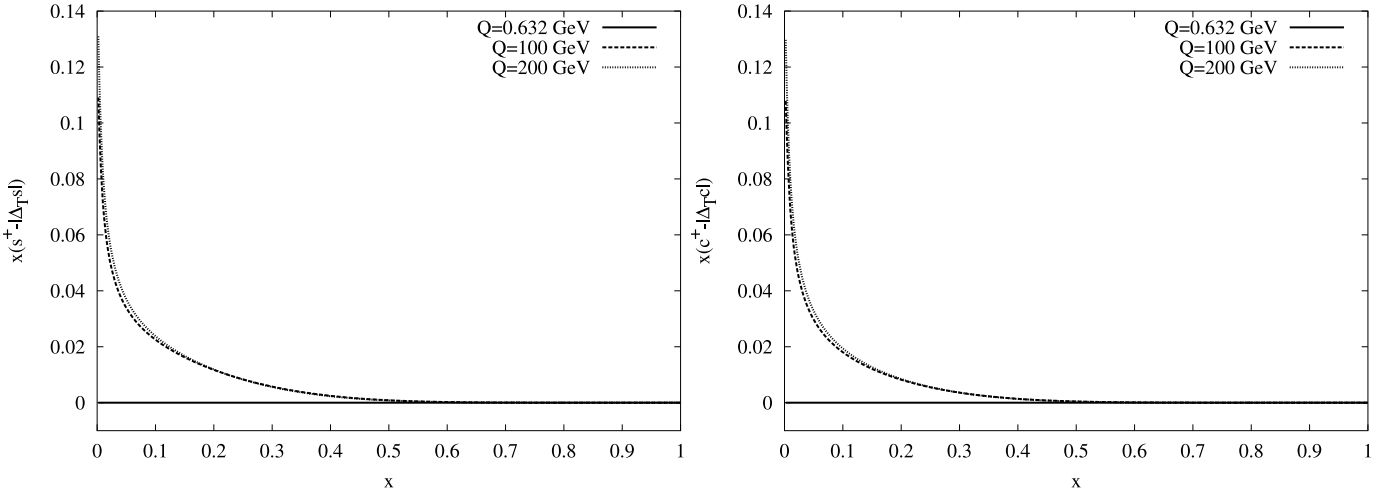

Figure 9: Soffer's inequality for strange and charm in the GRSV model.

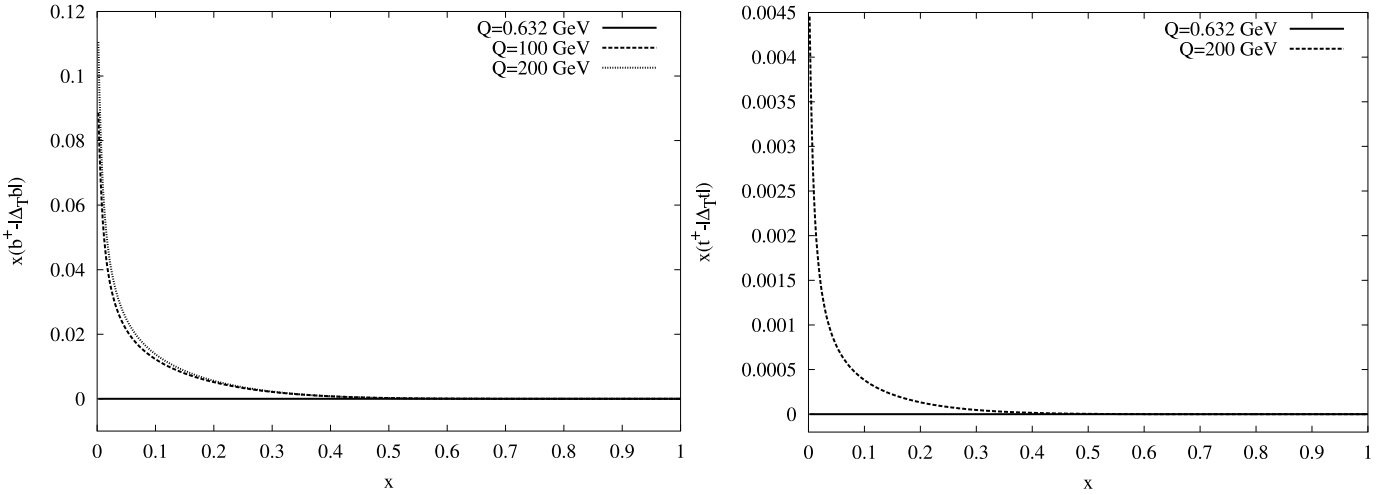

Figure 10: Soffer's inequality for bottom and top in the GRSV model.

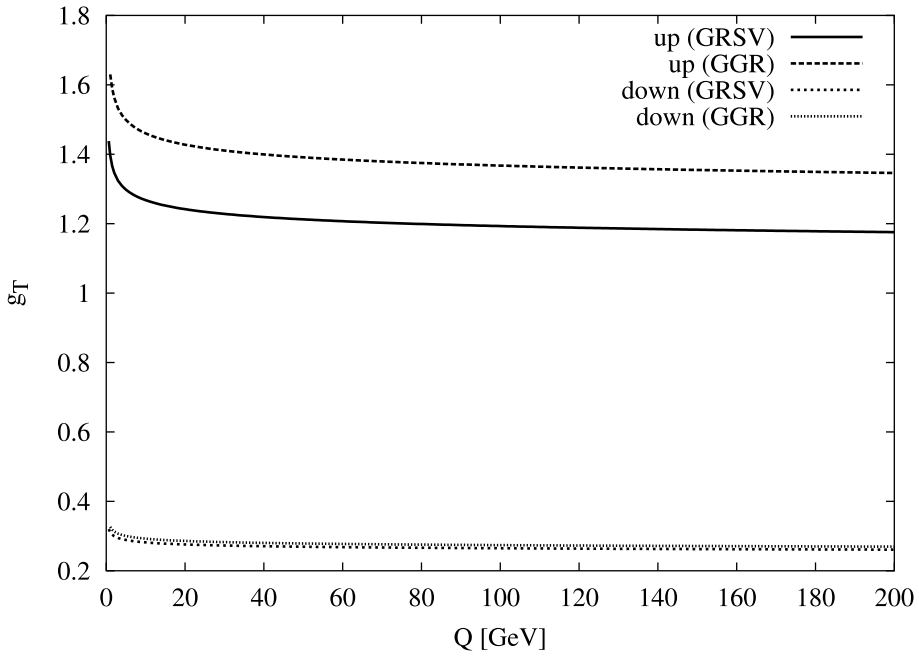

Figure 11: Tensor charge g_T as a function of Q for up and down quark for the GRSV and GGR models.